Composites Science and Technology 96 (2014) 97–102

Contents lists available at ScienceDirect

Composites Science and Technology

journal homepage: www.elsevier.com/locate/compscitech

Preparation and characterization of polymeric nanocomposites containing exfoliated tungstenite at high concentrations

Daniele Nuvoli [a], Mariella Rassu [a], Valeria Alzari [a], Roberta Sanna [a], Giulio Malucelli [b,*], Alberto Mariani [a,*]

[a] Dipartimento di Chimica e Farmacia, Università di Sassari, Local INSTM Unit, Via Vienna 2, 07100 Sassari, Italy
[b] Dipartimento di Scienza Applicata e Tecnologia, Politecnico di Torino, Sede di Alessandria, Local INSTM Unit, Viale T. Michel 5, 15121 Alessandria, Italy

ARTICLE INFO

Article history:
Received 25 September 2013
Received in revised form 27 January 2014
Accepted 17 March 2014
Available online 25 March 2014

Keywords:
A. Polymer–matrix composites (PMCs)
A. Nanoparticles
B. Thermal properties
B. Mechanical properties
D. Raman spectroscopy

ABSTRACT

For the first time, ultrasonication was exploited for obtaining tungstenite nanoparticles directly into a monomer (tetraethyleneglycol diacrylate) to be eventually polymerized without any further manipulation. The resulting liquid dispersions were characterized by Raman, transmission electron and scanning electron microscopies. Eventually, they were directly used for preparing nanocomposites containing a relatively large amount of exfoliated tungstenite. Differential scanning calorimetry and thermogravimetric analyses were performed in order to assess the effect of the presence of the exfoliated nanofiller on the thermal features of the polymer matrix: a clear improvement of the thermal and thermo-oxidative stability was observed. At variance, the effect of the exfoliated tungstenite on the glass transition temperature of the polymer matrix was negligible. Furthermore, the mechanical behavior of the obtained nanocomposites was evaluated by means of flexural and shore A hardness tests: the exfoliated nanofiller turned out to exert a strong reinforcing effect on the polymer matrix even at very low concentration.

1. Introduction

In the latest years, enormous scientific efforts have been done in order to seek for new methods to isolate, synthesize and apply new nanoparticles to advanced technologies. Among all, graphene has been largely studied; as known, it is a two-dimensional network of sp^2-hybridized carbon atoms exhibiting unique properties, partially related to its 2D nature, and a phenomenological behavior that can be exploited for a wide range of applications [1]. However, only more recently also other bidimensional nanomaterials have attracted the interest of the scientific community: among them, one of the most important classes is represented by transition metal dichalcogenides (TMDs). TMDs consist of hexagonal layers of metal atoms (M) sandwiched between two layers of chalcogen atoms (X) with MX_2 stoichiometry [2]. Analogously to graphite, the atoms in the layer are bound by strong covalent forces, while van der Waals interactions hold the layers together. In this context, monolayers of MoS_2 and WS_2 have received great attention because they are 2D semiconductor with tunable band gaps depending on size [3–5]. In particular, exfoliated WS_2 (EWS_2) was found to exhibit novel and superior properties with respect to the bulk structure, and hence such a nanomaterial has been used for the fabrication of catalysts [6], lubricants [7], lithium batteries [8], photoconductors [9], probes for scanning probe microscopy [10], shock absorbers [11], solar cell films [12]. The synthetic routes to prepare WS_2 nanomaterials include magnetron sputtering [13], thermal decomposition [14], laser ablation [12], chemical vapor deposition [15], sonochemical synthesis [16], hydrothermal/solvothermal routes [17,18] and mechanical activation [19]. However, the isolation of single atomic WS_2 layers is not easy because of their natural tendency to form fullerene-like, nanotube, or stacked multilayered geometries [20,21]. One of the most promising methods to produce 2D materials is the non-chemical liquid exfoliation by ultrasonication. This technique, initially developed for the obtainment of graphene [22], is based on the assumption that the energy required to exfoliate the layered material is balanced by the solvent-layer interaction when the solvent surface energy matches that of the nanomaterial to exfoliate. This route is very simple and allows avoiding the use of special apparatuses and any chemical manipulation that might introduce defects in the exfoliated structures. Liquid exfoliation was successfully used to obtain high concentration of graphene in liquid solvents [23–27] and reactive compounds [28–32]; some of these were employed to synthesize polymer nanocomposites [25,27,28,30–32]. Similarly, tungsten disulfide can be exfoliated to give single and few

* Corresponding authors. Tel.: +39 011 5644621 (G. Malucelli). Tel.: +39 079229556 (A. Mariani).
E-mail addresses: giulio.malucelli@polito.it (G. Malucelli), mariani@uniss.it (A. Mariani).

http://dx.doi.org/10.1016/j.compscitech.2014.03.015
0266-3538/

layered nanoparticles as reported by Coleman et al. [33] and Notley [34], who were able to disperse WS_2 in NMP and a surfactant, respectively.

This work aims to assess the use of EWS_2 as a new nanofiller in nanocomposite acrylic polymers and study its effect on the thermal and mechanical properties of the obtained materials. In addition, for the first time, an acrylic monomer (tetraethyleneglycol diacrylate, TEGDA) was used to exfoliate and disperse WS_2, instead of employing an inert solvent. Thus, the resulting dispersions were directly used for the preparation of the nanocomposite polymers without recovering the solid WS_2 nanoparticles, hence avoiding any possible restacking phenomenon. TEGDA was chosen because it has demonstrated an excellent ability to disperse and exfoliate tungsten disulfide; this monomer has been already used by our research group to obtain highly concentrated graphene dispersions and prepare the corresponding polymer nanocomposites [30,32].

2. Materials and methods

2.1. Materials

TEGDA (MW = 302.32, d = 1.11 g/ml) and WS_2 powder (particle size: 2 μm) were purchased from Sigma Aldrich and used as received without further purification. Trihexyltetradecylphosphonium persulfate (TETDPPS) was used as the radical initiator and was synthesized according to the procedure described in the literature [35].

2.2. Preparation of EWS_2 dispersions in TEGDA

Mixtures containing various amounts of tungstenite (0.1, 0.5, 1.0, 2.5 and 5.0 wt.%) in TEGDA (10 g) were put in a tubular plastic reactor (i.d. 15 mm) and placed in an ultrasonic bath (0.55 kW, water temperature 40 °C) for a selected time (0.5, 1.5, 2.5, 6.0, 12.5, 19.0 and 24.0 h). Finally, they were centrifuged for 30 min at 4000 rpm; the dark green liquid phase containing exfoliated WS_2 was recovered.

2.3. Characterization of EWS_2 dispersions

The concentration of EWS_2 was determined by filtration through polyvinylidene fluoride (PVDF) filters (pore size, 0.22 μm), in order to directly weigh the amount of EWS_2 dispersed.

UV–Vis spectroscopy measurements (Hitachi U-2010 spectrometer, 1 cm cuvette, λ = 630 nm [33]) were performed to find the actual tungstenite content in any diluted dispersion used for the nanocomposite preparation. To determine the absorption coefficient α from a known volume of initial dispersion, several dilutions were done and the absorbance was measured. The α value, which was found equal to 360 ml mg^{-1} m^{-1}, was calculated from absorbance vs. concentration plots.

Raman analyses were performed on EWS_2 flakes deposited on PVDF filters (see above) with a Bruker Senterra Raman microscope using an excitation wavelength of 532 nm at 0.5 mW. The spectra were acquired by averaging six acquisitions of 5 s with a 20× objective. For WS_2 powder, a laser power of 5 mW was used.

TEM analyses were performed with a ZEISS EM 109, operating at 80 kV. EWS_2 dispersion was washed three times with acetone, and the resulting TEGDA-free EWS_2 was deposited onto copper grids covered with a film of formware/carbon (300 mesh) and the solvent was evaporated.

SEM micrographies were obtained by using a SEM ZEISS DSM 962. Analyses were performed both on WS_2 powder and exfoliated tungstenite deposited on a silicon substrate.

2.4. Synthesis of TEGDA/EWS_2 nanocomposites

The masterbatch dispersion of EWS_2 in TEGDA was diluted with suitable amounts of this latter to achieve the desired concentration of exfoliated WS_2; then 0.5 mol% of TETDPPS were added and the mixture was homogenized. The polymerization reaction was performed in an oil bath at 80 °C for 1 h; DSC analysis performed on these samples showed residual polymerization peaks. Accordingly, the monomer conversion was completed by treating the samples in an oven at 100 °C for 48 h. DSC analyses on the post-cured samples showed a complete conversion.

2.5. Characterization of EWS_2 nanocomposites

Raman analysis on polymers were performed with a Bruker Senterra Raman microscope using an excitation wavelength of 532 nm at 5 mW. The spectra were acquired by averaging six acquisitions of 5 s with a 20× objective.

The surface hardness was measured on cylindrical samples (diameter = 22 mm, height = 5 mm) according to ASTM D2240 (Shore A) at 23 ± 2 °C. For each sample, five measurements were performed along different points, and the mean value was considered.

Differential Scanning Calorimetry (DSC) measurements were performed by means of a Q100 Waters TA Instruments calorimeter, equipped with TA Universal Analysis 2000 software, from −30 to 250 °C at a heating rate of 10 °C/min in inert atmosphere (nitrogen flow: 40 ml/min).

The thermal and thermo-oxidative stability of the materials was evaluated by thermogravimetric (TG) analyses using a Q500 TA analyzer. The measurements were performed placing the samples in open alumina pans (ca. 10 mg) in nitrogen or air atmosphere (gas flow: 60 ml/min) from 50 to 800 °C with a heating rate of 10 °C/min. In the followings, T_{10} and T_{max} are defined as the temperatures corresponding to 10% weight loss or to the maximum weight loss rate, respectively. The accuracy of the used thermogravimetric balance is ±1 °C on the temperature and ±1 wt.% on the weight, on the basis of the temperature and weight calibration. The measurements of each sample were repeated twice in order to ensure reproducible data.

The surface morphology of the samples was investigated using a Scanning Electron Microscope (SEM, LEO 1450VP). The specimens were fractured in liquid nitrogen, fixed to conductive adhesive tapes and gold-metallized.

Three point bending flexural tests, according to ASTM D790, were performed, using a Zwick–Roll Z010 apparatus, equipped with a 5 kN load cell, 30 mm support span, at 23 ± 2 °C and 50 ± 5% relative humidity. At least five tests were repeated for each material in order to have reproducible and significant data.

3. Results and discussion

First of all, the best conditions to obtain high concentrations of EWS_2 dispersed in TEGDA were investigated.

As described in the Experimental, the adopted procedure to obtain dispersions is extremely simple and envisages the direct sonication of tungsten disulfide powder in TEGDA without any chemical manipulation.

A preliminary test usually confirming the nanometric dimensions of the dispersed particles was the occurrence of the Tyndall effect [36] (not shown).

In a first series of experiments, keeping constant the sonication time, a study on the effect of initial WS_2 concentration on the resulting concentration of exfoliated tungstenite EWS_2 was carried out. In particular, five dispersions containing from 0.1 to 5.0 wt.%

WS_2 powder were prepared, and the sonication time was kept constant at 6 h (Fig. 1a). EWS_2 concentration increases considerably with the concentration of initial WS_2 powder, from 0.042 mg/ml (for 0.1 wt.% WS_2) to 3.30 mg/ml (for 5.0 wt.% WS_2).

A second series of experiments was performed in order to study the effect of sonication time on the concentration of exfoliated tungstenite. In this case, seven dispersions containing 5 wt.% of WS_2 powder were prepared, and put into the sonication bath for increasing times, from 0.5 to 24.0 h. As depicted in Fig. 1b, EWS_2 concentration increases with sonication time, ranging from 1.05 mg/ml, for 30 min of ultrasound application, to over 6.30 mg/ml for 24 h of sonication time.

As can be seen by comparing data in Fig. 1, the initial WS_2 concentration has a stronger influence on the amount of EWS_2 dispersed with respect to sonication time, thus indicating that the exfoliation process occurs more easily with respect to graphene dispersed in the same monomer [26].

On the basis of these data, the best conditions for the obtainment of the highest amount of EWS_2 can be summarized as follows: 24 h sonication time and 5.0 wt.% initial WS_2 powder concentration in TEGDA.

It is noteworthy that the EWS_2 concentration obtained in TEGDA was considerably higher than other concentrations found by non-chemical liquid exfoliation methods. Indeed, in these latter cases, a maximum concentration of 0.04 mg/ml was found. [33,34,37].

SEM and TEM analyses were performed to investigate the morphology of EWS_2 particles dispersed in TEGDA. Fig. 2 shows the typical SEM micrographs of the pristine WS_2 powder compared with that of exfoliated WS_2. WS_2 powder shows the typical structure of a layered material, with aggregated micrometric flakes. The exfoliation process, which involves ultrasonication, significantly reduces the dimensions of the flakes, which become nanometric. This finding was further confirmed by TEM analyses (Fig. 3); the corresponding micrographs indicate that the typical observed flakes have an average lateral size within 100–200 nm and consist of few layers. In any case, WS_2 aggregates attributable to unexfoliated material were not observed.

Furthermore, it should be noticed here that AFM cannot be always used in order to characterize the dispersions of graphene-like materials. Indeed, it was demonstrated that this technique is not a reliable method if applied to graphene obtained by liquid exfoliation in highly-boiling liquids. As a matter of the fact, when graphene is obtained by liquid exfoliation, AFM largely overestimates the height of the steps because of the presence of a large number of solvent layers among those of graphene. For this reason, since TEGDA is not only a highly boiling liquid, but also a monomer, which may polymerize upon heating, AFM was not used in this work [38].

Raman spectroscopy is a basic characterization technique for 2D materials as shifts in peak positions and peak shapes give much information on the structure of the materials, in particular referring to the number of layers and the presence of defects in the structure [39]. Fig. 4 shows the Raman spectra of the pristine WS_2 powder and of the exfoliated material deposited onto a PVDF filter.

The spectra of the pristine WS_2 powder and of exfoliated EWS_2 are both characterized by two main peaks. These have been discussed in detail by many researchers: the first major peak at around 350 cm^{-1} is assigned at the E_{2g} mode for the motion of W + S atoms in the *x*–*y* layered plane, while the second peak at ca. 420 cm^{-1} is assigned at the A_{1g} mode for the motion of two S atoms along the *z*-axis of the unit cell. In particular, the WS_2 powder used in this work showed the E_{2g} peak at 350.0 cm^{-1} and the A_{1g} peak at 418.5 cm^{-1}. The spectrum of exfoliated WS_2 showed a blue shift of both peaks with respect to WS_2 powder peaks: namely, E_{2g} peak shifts to 352.5 cm^{-1} and A_{1g} peak shifts to 421.0 cm^{-1}. In addition, the E_{2g} peak is more intense and broader if compared with the analogue peak of bulk WS_2. The blue shift

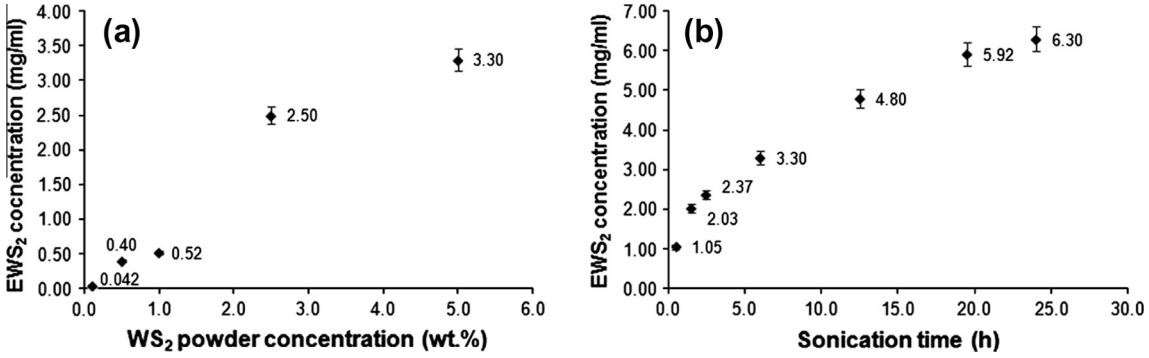

Fig. 1. EWS_2 concentration as a function of initial WS_2 powder concentration (a) and sonication time (b).

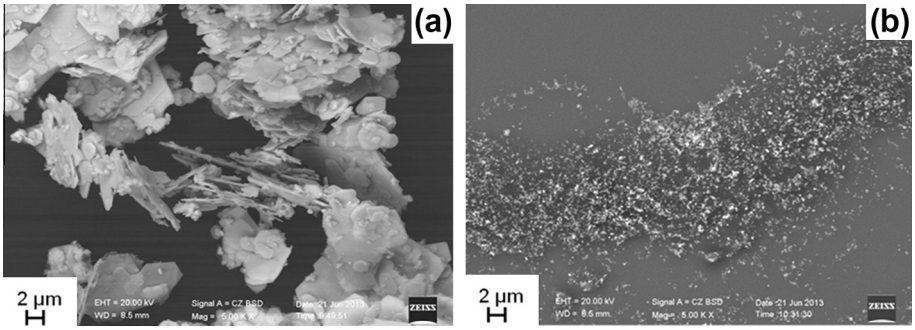

Fig. 2. SEM micrographs of pristine WS_2 powder (a), and EWS_2 deposited on a silicon substrate (b).

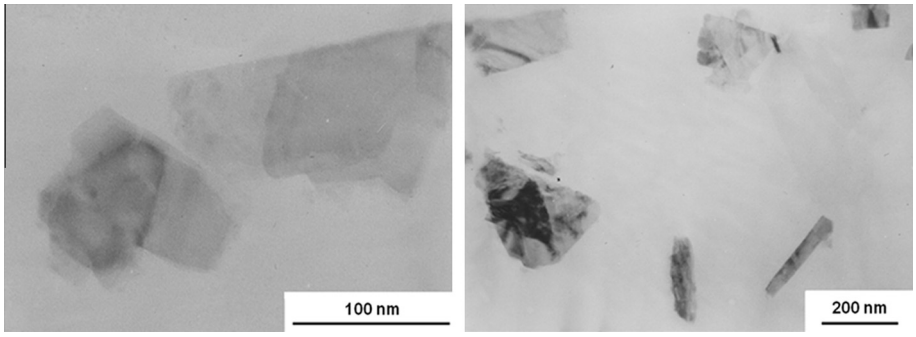

Fig. 3. TEM micrographs of EWS_2 dispersed in TEGDA.

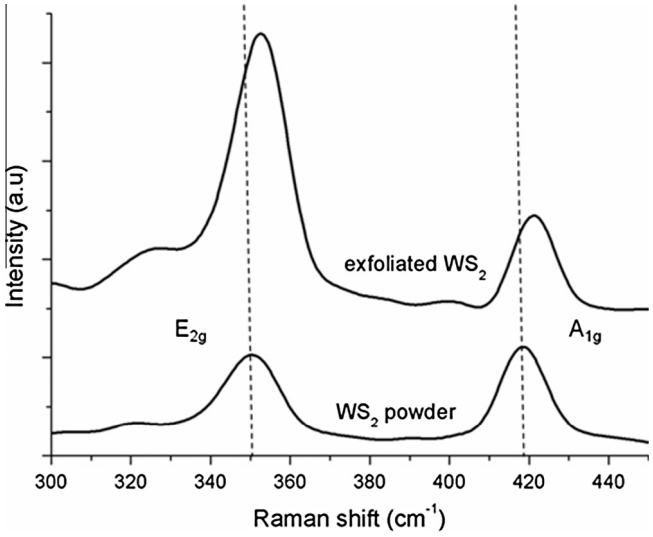

Fig. 4. Raman spectrum of EWS_2 compared with the spectrum of the pristine WS_2 powder.

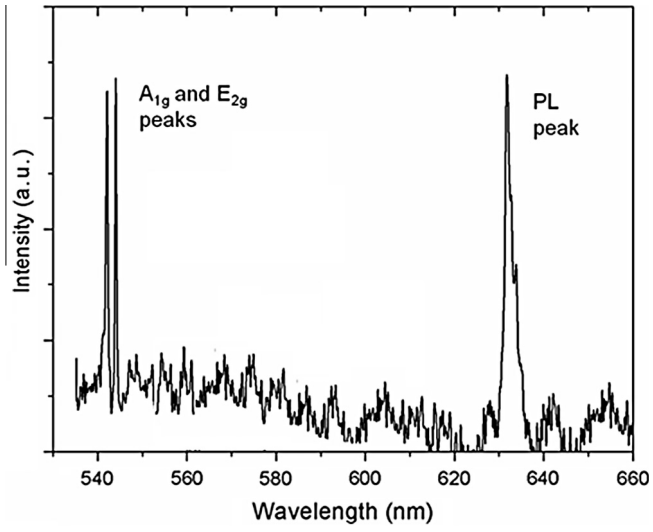

Fig. 5. PL peak for EWS_2 deposited on a PVDF filter.

can be explained in terms of reduction of interlayer interaction [34,40], while the broadening of the peak at ca. 350 cm^{-1} is ascribed to the phonon confinement within the single layer, and proves that the lateral dimensions of the particle are in the nanometer range [40,41].

Recently, some studies related to Raman analysis of WS_2 an MoS_2 demonstrated that these nanomaterials give rise to photoluminescence (PL), the intensity of which increases with decreasing the thickness of the particles [3,42]. In particular, for a monolayer, the PL is very intense and is due to the direct excitonic transition at the K point. Increasing the number of layers, the indirect transition between the local minimum of the conduction band at the *T* point and the local maximum of the valence band at the Γ point compete with the direct transition at the *K* point, which dramatically reduces the PL. In Fig. 5, the PL peak (632 nm) of EWS_2 is shown: as can be seen, this peak is not very intense and shows the same magnitude order of A_{1g} and E_{2g} peaks, thus indicating that only a little part of EWS_2 is as single layer.

Table 1
List of poly(TEGDA)/EWS_2 nanocomposites prepared by varying the EWS_2 content.

Sample	EWS_2 concentration in TEGDA (mg/ml)	Dilution factor[a]	EWS_2 concentration in poly(TEGDA) (wt.%)
B0	0	–	0
B1	0.063	1:100	0.0057
B2	0.10	1:60	0.0090
B3	0.52	1:12	0.048
B4	1.05	1:6	0.095
B5	2.10	1:3	0.19
B6	6.30	–	0.57

[a] Referred to the masterbatch dispersion (conc. 6.30 mg/ml).

Pursuing this research, we focused on the preparation of EWS_2/TEGDA nanocomposites. It is noteworthy that the masterbatch dispersion in the acrylic monomer was directly used to obtain the resulting nanocomposites without any further common process (i.e. solvent removal, filtration, mixing, etc.): to the best of our knowledge, this is the first example of a polymer nanocomposite containing EWS_2 directly dispersed into an acrylic monomer. Indeed, the direct polymerization of the dispersion avoids any process that can lead to the reaggregation of WS_2 and is advantageous in terms of time and costs.

For this purpose, several TEGDA-based nanocomposites were prepared by varying EWS_2 concentration from 0 to 0.57 wt.% (Table 1), by properly diluting the TEGDA masterbatch dispersion (exfoliated WS_2 concentration: 6.30 mg/ml).

In order to verify the effective dispersion of EWS_2 into the polymer matrix and its non-reaggregation, Raman analysis was performed on the polymer nanocomposites.

In Fig. 6, the Raman spectrum of the EWS_2 – containing nanocomposite is compared with that of EWS_2. The position and shape of E_{2g} and A_{1g} peaks are very similar and confirm the non-reaggregation of EWS_2 during the polymerization process, and hence the obtainment of a real nanocomposite.

The surface morphology of nanocomposites was investigated by SEM analysis. As depicted in Fig. 7, there are no significant differences between neat poly(TEGDA) and the polymers filled with different amounts of EWS_2: for all the samples, the surface appears

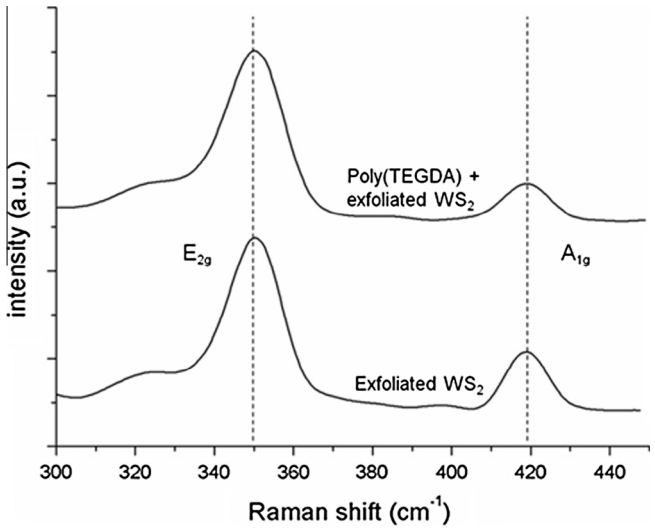

Fig. 6. Comparison between Raman signals of EWS_2 dispersed in the poly(TEGDA) matrix and EWS_2 deposited on PVDF filter.

completely smooth and EWS_2 nanoparticles dispersed into the polymer matrix are not visible. This finding further confirms that exfoliated tungstenite is homogeneously dispersed into poly(TEGDA) and WS_2 aggregates are not present in the nanocomposites.

The thermal and thermo-oxidative stability of the samples and the effect of the presence of exfoliated WS_2 were investigated by TGA analysis in nitrogen and air, respectively; the results are listed in Table 2.

In nitrogen, the thermal stability of poly(TEGDA) is affected by the presence of EWS_2: indeed, T_{10} and T_{max1} values of the pure poly(TEGDA) shift toward higher temperatures in presence of the nanofiller. In particular, moving from the pure polymer matrix to the nanocomposites, the T_{10} values increase is around 15 °C, regardless of the amount of EWS_2 used. A similar trend is observed for T_{max1}, with the only exception of the sample containing the largest amount of EWS_2, in which the effect of the nanofiller is more evident and T_{max1} increases up to 431 °C.

In air, the degradation of the nanocomposites occurs in a two-step process; for each step, the trend of T_{10} and T_{max} values is very similar to that described in nitrogen: once again, the effect of EWS_2 is particularly evident for sample B6, with an increase of 25 °C for T_{max1} and of 50 °C for T_{max2}.

DSC scans were performed to assess the completeness of the curing reaction, as well as to evaluate the glass transition temperature (T_g) of all the samples: the obtained data are collected in Table 3. All the DSC thermograms do not show any exothermal phenomena, thus indicating that the experimental parameters chosen for performing the curing process are able to ensure the completeness of the reaction, regardless of the presence and of the amount of nanofiller. In addition, the presence of exfoliated WS_2 does not practically influence T_g (and therefore the crosslinking density of the cured network), which is stable around 44 °C. A similar behavior has been already observed for graphene nanocomposites [32,43,44].

As far as the mechanical behavior is considered, flexural and shore A hardness tests have been carried out both on pure poly(TEGDA) and on its nanocomposites. The obtained data, listed in Table 3, clearly indicate that exfoliated tungstenite exerts a strong reinforcing effect on the polymer matrix even at very low concentration; indeed, the flexural modulus increases with increasing EWS_2 concentration, reaching a maximum for sample B6, with an increase of 30% with respect to the pure polymer matrix. In addition, the presence of exfoliated tungstenite determines a slight increase of the surface hardness of the nanocomposites, as compared to pure poly(TEGDA).

It should be highlighted that in an analogous work devoted to investigate the effect of graphene content on the mechanical properties of a poly(TEGDA) nanocomposite, we found a different behavior. Indeed, a reinforcing effect for low nanofiller loadings until a threshold value of concentration (4.67 mg/ml) was achieved [28]. Beyond this value, the mechanical properties were found to worsen. This threshold behavior in graphene-containing polymer nanocomposite was also assessed for other systems and can be

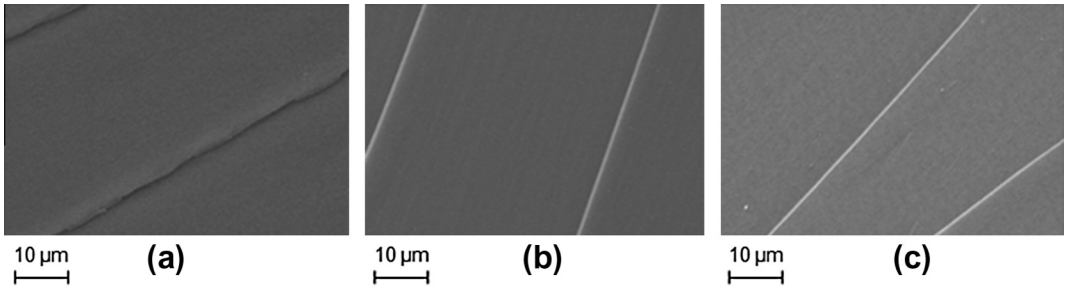

Fig. 7. SEM micrographs of poly(TEGDA) nanocomposites: neat polymer (a, sample B0) and polymers with 0.048 wt.% (b, sample B3) and 0.57 wt.% (c, sample B6) EWS_2.

Table 2
TGA data of poly(TEGDA) and of its nanocomposites containing EWS_2.

Sample	Nitrogen			Air			
	T_{10} (°C)	T_{max1} (°C)	Residue (%)	T_{10} (°C)	T_{max1} (°C)	T_{max2} (°C)	Residue (%)
B0	360	399	3.4	359	406	520	0.4
B1	374	418	3.5	359	416	534	0.5
B2	376	417	3.6	359	412	545	0.6
B3	370	418	4.4	360	413	540	0.7
B4	371	409	4.6	356	413	537	0.8
B5	370	411	4.9	370	406	537	0.8
B6	374	431	6.7	369	429	568	0.9

Table 3
Glass transition temperature, flexural modulus and shore A hardness values for poly(TEGDA) and its nanocomposites.

Sample	T_g (°C)[a]	Flexural modulus (MPa)	Hardness – shore A
B0	44	745±32	87.6±0.5
B1	42	740±30	92.0±0.6
B2	40	871±23	93.0±0.6
B3	41	909±28	93.0±0.5
B4	42	980±24	92.5±1.5
B5	49	1030±21	90.5±0.5
B6	44	1051±27	90.1±0.7

[a] (N ± 0.5).

attributable to the sliding of one graphene layer over the other [25,28,30,31]. However, graphene and EWS_2 nanocomposites cannot be easily compared in that many other factors should be taken into account.

4. Conclusions

Exfoliated tungstenite/TEGDA dispersions were successfully prepared by exploiting a simple sonication method without any chemical manipulation, as assessed by scanning electron and transmission electron microscopies and Raman spectroscopy. The liquid dispersions were directly used for preparing nanocomposites without recovering the solid WS_2 nanoparticles, hence avoiding any possible restacking phenomenon and simplifying the protocol commonly used. The thermal and mechanical properties of the obtained nanomaterials were investigated: the presence of the exfoliated nanofiller turned out to exert a strong reinforcing effect on the polymer matrix even at very low concentration, as clearly indicated by flexural tests. Furthermore, a slight increase of the shore A hardness was observed. The nanofiller was also responsible for a significant enhancement of the thermal and thermo-oxidative stability of the polymer matrix, as assessed by thermogravimetric analyses. At variance, the nanofiller did not substantially affect the glass transition temperature of the polymer, which was around ca. 44 °C.

References

[1] Singh V, Joung D, Zhai L, Das S, Khondaker SI, Seal S. Graphene based materials: past, present and future. Prog Mater Sci 2011;56:1178–271.
[2] Ataca C, Şahin H, Ciraci S. Stable, single-layer MX_2 transition-metal oxides and dichalcogenides in a honeycomb-like structure. J Phys Chem C 2012;116:8983–99.
[3] Mak KF, Lee C, Hone J, Shan J, Heinz TF. Atomically thin MoS_2: a new direct-gap semiconductor. Phys Rev Lett 2010;105:136805–8.
[4] Albe K, Klein A. Density-functional-theory calculations of electronic band structure of single-crystal and single-layer WS_2. Phys Rev B 2002;66:073413–73415.
[5] Ma YD, Dai Y, Guo M, Niu CW, Lu JB, Huang BB. Electronic and magnetic properties of perfect, vacancy-doped, and nonmetal adsorbed $MoSe_2$, $MoTe_2$ and WS_2 monolayers. Phys Chem Chem Phys 2011;13:15546–53.
[6] Chianelli RR, Berhault G, Torres B. Unsupported transition metal sulfide catalysts: 100 years of science and application. Catal Today 2009;147:275–86.
[7] Rapoport L, Moshkovich A, Perfilyev V, Tenne R. On the efficacy of IF–WS_2 nanoparticles as solid lubricant: the effect of the loading scheme. Tribol Lett 2007;28:81–7.
[8] Feng C, Huang L, Guo Z, Liu H. Synthesis of tungsten disulfide (WS_2) nanoflakes for lithium ion battery application. Electrochem Commun 2007;9:119–22.
[9] Ballif C, Regula M, Levy F. Optical and electrical properties of semiconducting WS_2 thin films: from macroscopic to local probe measurements. Sol Energy Mater Sol Cells 1999;57:189–207.
[10] Rothschild A, Cohen SR, Tenne R. WS_2 nanotubes as tips in scanning probe microscopy. Appl Phys Lett 1999;75:4025–7.
[11] Zhu YQ, Sekine T, Li YH, Wang WX, Fay MW, Edwards H, et al. WS_2 and MoS_2 inorganic fullerenes—super shock absorbers at very high pressures. Adv Mater 2005;17:1500–3.
[12] Ellmer K. Preparation routes based on magnetron sputtering for tungsten disulfide (WS_2) films for thin-film solar cells. Phys Stat Sol (b) 2008;245:1745–60.
[13] Margulis L, Salitra G, Tenne R, Talianker M. Nested fullerene-like structures. Nature 1993;365:113–4.
[14] Remskar M, Skraba Z, Regula M, Ballif C, Sanjines R, Levy F. New crystal structures of WS_2: microtubes, ribbons, and ropes. Adv Mater 1998;10:246–9.
[15] Zelenski CM, Dorhout PK. Template synthesis of near-monodisperse microscale nanofibers and nanotubules of MoS_2. J Am Chem Soc 1998;120:734–42.
[16] Hu JJ, Zabinski JS, Sanders JH, Bultman JE, Voevodin AA. Pulsed laser syntheses of layer-structured WS_2 nanomaterials in water. J Phys Chem B 2006;110:8914–6.
[17] Pol VG, Pol SV, George PP, Gedanken A. Combining MoS_2 or $MoSe_2$ nanoflakes with carbon by reacting $Mo(CO)_6$ with S or Se under their autogenic pressure at elevated temperature. J Mater Sci 2008;43:1966–73.
[18] Dhas NA, Suslick KS. Sonochemical preparation of hollow nanospheres and hollow nanocrystals. J Am Chem Soc 2005;127:2368–9.
[19] Li YD, Li XL, He RR, Zhu J, Deng ZX. Artificial lamellar mesostructures to WS_2 nanotubes. J Am Chem Soc 2002;124:1411–9.
[20] Wu JF, Fu X. A low-temperature solvothermal method to prepare hollow spherical WS_2 nanoparticles modified by TOA. Mater Lett 2007;61:4332–5.
[21] Wu Z, Wang D, Zan X, Sun A. Synthesis of WS_2 nanosheets by a novel mechanical activation method. Mater Lett 2010;64:856–8.
[22] Hernandez Y, Nicolosi V, Lotya M, Blighe FM, Sun Z, De S, et al. High-yeld production of graphene by liquid-phase exfoliation of graphite. Nat Nantechnol 2008;3:563–8.
[23] Khan U, O'Neill A, Lotya M, De S, Coleman JN. High-concentration solvent exfoliation of graphene. Small 2010;6:864–71.
[24] Lotya M, King PJ, Khan U, De S, Coleman JN. High-concentration, surfactant-stabilized graphene dispersions. ACS Nano 2010;4:3155–62.
[25] Alzari V, Nuvoli D, Scognamillo S, Piccinini M, Gioffredi E, Malucelli G, et al. Graphene-containing nanocomposite hydrogels of poly(*N*-isopropylacrylamide) prepared by frontal polymerization. J Mater Chem 2011;21:8727–33.
[26] Nuvoli D, Valentini L, Alzari V, Scognamillo S, Bittolo Bon S, Piccinini M, et al. High concentration few-layer graphene sheets obtained by liquid phase exfoliation of graphite in ionic liquid. J Mater Chem 2011;21:3428–31.
[27] Alzari V, Nuvoli D, Sanna R, Peponi L, Piccinini M, Bittolo Bon S, et al. Multistimuli-responsive hydrogels of poly(2-acrylamido-2-methyl-1-propanesulfonic acid) containing graphene. Colloid Polym Sci 2013. http://dx.doi.org/10.1007/s00396-013-2978-.
[28] Alzari V, Nuvoli D, Sanna R, Scognamillo S, Piccinini M, Kenny JM, et al. In situ production of high filler content graphene-based polymer nanocomposites by reactive processing. J Mater Chem 2011;21:16544–9.
[29] Nuvoli D, Alzari V, Sanna R, Scognamillo S, Piccinini M, Peponi L, et al. The production of concentrated dispersions of few-layer graphene by the direct exfoliation of graphite in organosilanes. Nanoscale Res Lett 2012;7:674–80.
[30] Scognamillo S, Gioffredi E, Piccinini M, Lazzari M, Alzari V, Nuvoli D, et al. Synthesis and characterization of nanocomposites of thermoplastic polyurethane with both graphene and graphene nanoribbon fillers. Polymer 2012;53:4019–24.
[31] Sanna R, Sanna D, Alzari V, Nuvoli D, Scognamillo S, Piccinini M, et al. Synthesis and characterization of graphene-containing thermoresponsive nanocomposite hydrogels of poly(N-vinylcaprolactam) prepared by frontal polymerization. J Pol Sci Part A Polym Chem 2012;50:4110–8.
[32] Nuvoli D, Alzari V, Sanna R, Scognamillo S, Alongi J, Malucelli G, et al. Synthesis and characterization of graphene-based nanocomposites with potential use for biomedical applications. J Nanopart Res 2013;15:1512–9.
[33] Coleman JN, Lotya M, O'Neill A, Bergin SD, King PJ, Khan U, et al. Two-dimensional nanosheets produced by liquid exfoliation of layered materials. Science 2011;331:568–71.
[34] Notley SM. High yield production of photoluminescent tungsten disulphide nanoparticles. J Colloid Interface Sci 2013;396:160–4.
[35] Mariani A, Nuvoli D, Alzari V, Pini M. Phosphonium-based ionic liquids as a new class of radical initiators and their use in gas-free frontal polymerization. Macromolecules 2008;41:5191–6.
[36] Li D, Müller MB, Gilje S, Kaner RB, Wallace GG. Processable aqueous dispersions of graphene nanosheets. Nat Nanotechnol 2008;3:101–5.
[37] Zhou KG, Mao NN, Wang HX, Peng Y, Zhang HL. Mixed-solvent strategy for efficient exfoliation of inorganic graphene analogues. Angew Chem Int Ed 2011;50:10839–42.
[38] Hernandez Y, Lotya M, Rickard D, Bergin SD, Coleman JN. Measurement of multicomponent solubility parameters for graphene facilitates solvent discovery. Langmuir 2009;26:3208–13.
[39] Ferrari AC. Raman spectroscopy of graphene and graphite: Disorder, electron–phonon coupling, doping and nonadiabatic effects. Solid State Commun 2007;143:47–57.
[40] Ramakrishna Matte HSS, Gomathi A, Manna AK, Late DJ, Datta R, Pati SK, et al. MoS_2 and WS_2 analogues of graphene. Angew Chem Int Ed 2010;49:4059–62.
[41] Frey GL, Tenne R, Matthews MJ, Dresselhaus MS, Dresselhaus G. Raman and resonance Raman investigation of MoS_2 nanoparticles. Phys Rev B 1999;60:2883–92.
[42] Splendiani A, Sun L, Zhang Y, Li T, Kim J, Chim CY, et al. Emerging photoluminescence in monolayer MoS_2. Nano Lett 2010;10:1271–5.
[43] Ansari S, Giannelis EP. Functionalized graphene sheet poly(vinylidene fluoride) conductive nanocomposites. J Polym Sci Part B Polym Phys 2009;47:888–9.
[44] Garboczi EJ, Snyder KA, Douglas JF, Thorpe MF. Geometrical percolation-threshold of overlapping ellipsoids. Phys Rev E 1995;52:819–28.